THE JOURNAL OF BIOLOGICAL CHEMISTRY
Vol. 276, No. 39, Issue of September 28, pp. 36809–36816, 2001

Printed in U.S.A.

Characterization of *SH2D1A* Missense Mutations Identified in X-linked Lymphoproliferative Disease Patients*

Received for publication, February 9, 2001, and in revised form, July 12, 2001
Published, JBC Papers in Press, July 26, 2001, DOI 10.1074/jbc.M101305200

Massimo Morra,[a,b,c] Maria Simarro-Grande,[a,d] Margarita Martin,[e] Alice Siau-In Chen,[a] Arpad Lanyi,[f] Olin Silander,[a] Silvia Calpe,[a] Jack Davis,[f] Tony Pawson,[g] Michael J. Eck,[h] Janos Sumegi,[f] Pablo Engel,[e] Shun-Cheng Li,[i,j] and Cox Terhorst[a,b]

From the [a]Division of Immunology, Beth Israel Deaconess Medical Center and the [h]Department of Cancer Biology, Dana-Farber Cancer Institute, Harvard Medical School, Boston, Massachusetts 02215, the [e]Department of Cellular Biology and Pathology, Faculty of Medicine, University of Barcelona, Barcelona 08036, Spain, the [f]Department of Pathology and Microbiology, University of Nebraska Medical Center, Omaha, Nebraska 68198, the [g]Samuel Lunenfeld Research Institute, Mount Sinai Hospital and Department of Molecular and Medical Genetics, University of Toronto, Toronto, Ontario M5G1X5, Canada, and the [i]Department of Biochemistry, Faculty of Medicine and Dentistry, University of Western Ontario, London, Ontario N6A5C1, Canada

X-linked lymphoproliferative disease (XLP) is a primary immunodeficiency characterized by extreme susceptibility to Epstein-Barr virus. The XLP disease gene product *SH2D1A* (SAP) interacts via its SH2 domain with a motif (TIY*XX*V) present in the cytoplasmic tail of the cell-surface receptors CD150/SLAM, CD84, CD229/Ly-9, and CD244/2B4. Characteristically, the SH2D1A three-pronged interaction with Tyr^{281} of CD150 can occur in absence of phosphorylation. Here we analyze the effect of SH2D1A protein missense mutations identified in 10 XLP families. Two sets of mutants were found: (i) mutants with a marked decreased protein half-life (*e.g.* Y7C, S28R, Q99P, P101L, V102G, and X129R) and (ii) mutants with structural changes that differently affect the interaction with the four receptors. In the second group, mutations that disrupt the interaction between the SH2D1A hydrophobic cleft and Val +3 of its binding motif (*e.g.* T68I) and mutations that interfere with the SH2D1A phosphotyrosine-binding pocket (*e.g.* C42W) abrogated SH2D1A binding to all four receptors. Surprisingly, a mutation in SH2D1A able to interfere with Thr −2 of the CD150 binding motif (mutant T53I) severely impaired non-phosphotyrosine interactions while preserving unaffected the binding of SH2D1A to phosphorylated CD150. Mutant T53I, however, did not bind to CD229 and CD224, suggesting that SH2D1A controls several critical signaling pathways in T and natural killer cells. Because no correlation is present between identified types of mutations and XLP patient clinical presentation, additional unidentified genetic or environmental factors must play a strong role in XLP disease manifestations.

X-linked lymphoproliferative (XLP)[1] disease is an immune disorder characterized by an extreme vulnerability to Epstein-Barr virus (EBV) (1–7). Fatal infectious mononucleosis, dysgammaglobulinemia, and malignant lymphoma are the major XLP phenotypes (1). Although XLP patients can develop dysgammaglobulinemia and B cell lymphomas after an EBV infection, a causal relationship between the virus and these XLP phenotypes has not been established. Indeed, immunoglobulin deficiencies and B cell non-Hodgkin's lymphomas have now been observed in XLP patients who were sero- and/or polymerase chain reaction-negative for EBV (8–10). Patients infected with EBV mount an uncontrolled polyclonal expansion of T and B cells that leads to death through hepatic necrosis and bone marrow failure (1). NK cell dysfunctions are detected in some (but not all) XLP patients (11–14).

The XLP gene encodes a 128-residue protein (SAP or SH2D1A), which comprises an SH2 domain and a C-terminal 26-amino acid tail (15–17). The SH2D1A SH2 domain, expressed in the cytoplasm of T, NK, and possibly B cells (18), binds to a consensus motif in the cytoplasmic tail of CD150 (16), CD244 (11, 13, 19, 20), and CD229 and CD84 (21, 22). These glycoproteins are members of the CD150 family (5, 23) and are expressed on a variety of hematopoietic cells. CD150 is found on CD45RO^{high} memory T cells, immature thymocytes, a small fraction of B cells, and activated dendritic cells and is rapidly up-regulated upon activation of T, B, and dendritic cells (24). Anti-CD150 antibodies are also particularly effective in inducing interferon-γ by both Th1 clones and mitogen-activated human or mouse T lymphocytes (25, 26). Importantly, SH2D1A has been shown to block recruitment of the SHP-2 phosphatase to the tail of phosphorylated CD150 (16). As CD150 is a self-ligand, it is thought to be involved in T/B cell interactions and is therefore relevant to a model for pathogenesis of XLP (5, 16, 24, 27). CD150 was also recently identified as another receptor for the measles virus (28).

CD244 is an *N*-glycosylated protein predominantly expressed on NK cells, γδ T cells, monocytes, and a subset of CD8$^+$ T cells (29). The high affinity between CD244 and its ligand CD48 (30, 31) is of particular relevance to NK and CD8$^+$ T cell responses in XLP because CD48 is one of the major

* This work was supported in part by National Institutes of Health Grant PO1-AI-35714 (to C. T.) and by grants from the National Foundation March of Dimes (to C. T.) and the National Cancer Institute of Canada (to S.-C. L.). The costs of publication of this article were defrayed in part by the payment of page charges. This article must therefore be hereby marked "*advertisement*" in accordance with 18 U.S.C. Section 1734 solely to indicate this fact.

The nucleotide sequence(s) reported in this paper has been submitted to the GenBank™/EBI Data Bank with accession number(s) AF322912 and AF322913.

[b] To whom correspondence should be addressed: Div. of Immunology, RE-204, Beth Israel Deaconess Medical Center, Harvard Medical School, 330 Brookline Ave., Boston, MA 02215. Tel.: 617-667-7147; Fax: 617-667-7140; E-mail: terhorst@caregroup.harvard.edu and mmorra@caregroup.harvard.edu.

[c] Supported by an American-Italian Cancer Foundation fellowship.
[d] Supported by a fellowship from the Ministerio de Educacion y Cultura of Spain.
[j] Research Scientist of the National Cancer Institute of Canada.

[1] The abbreviations used are: XLP, X-linked lymphoproliferative disease; EBV, Epstein-Barr virus; WT, wild-type; GST, glutathione *S*-transferase; CHAPS, 3-[(3-cholamidopropyl)dimethylammonio]-1-propanesulfonic acid; NK, natural killer; SHP, SH2 domain-containing protein tyrosine phosphatase.

receptors up-regulated on B cells following EBV transformation. Moreover, a defect in NK cell-mediated cytotoxicity in some XLP patients was attributed to dysfunctional signaling by CD244 (11, 12, 14).

SH2D1A has recently been shown to interact with a 62-kDa adapter, Dok1 ($p62^{dok}$) (32). Dok1 is present in hematopoietic cells, where Dok1 constitutively associates with the $p120^{Ras}$ GTPase-activating protein (32).

Classically, high affinity association of SH2 domains with Tyr-containing motifs (i) depends upon phosphorylation of the Tyr in the ligand and (ii) requires that the Tyr(P) be embedded within a specific amino acid sequence, where an additional contact C-terminal (usually at position +3) to the Tyr(P) is established. To bind to the non-phosphorylated CD150 Tyr^{281} motif, the SH2 domain of SH2D1A uses a "three-pronged" modality of binding instead of a conventional "two-pronged" recognition (16, 33, 34). The SH2D1A structure characteristically includes a central β sheet with α helices packed against either side (33). The additional interactions of SH2D1A involve the side chains of residues −2 and −1 (Thr^{279} and Ile^{280}) adjacent to Tyr^{281} in the CD150 peptide. These interact with residues in the βD strand of the SH2 domain (33). The SH2D1A-binding motif TIpY*XX*V is also found in the cytoplasmic domains of CD229 and CD84 (35, 36).

Several classes of *SH2D1A* mutations have so far been identified in XLP patients: (*a*) micro/macrodeletions, (*b*) mutations interfering with mRNA transcription or splicing, and (*c*) nonsense mutations or amino acid substitutions. Because missense mutations spanning the entire *SH2D1A* coding sequence have been identified in XLP patients (9, 15, 16, 37), SH2D1A provides a unique model to study structure/function relationships in an SH2 domain.

Here, we analyze a series of SH2D1A proteins with missense mutations by *in vitro* and *in vivo* studies. We report differential binding of these mutants to the hematopoietic cell receptors CD150, CD244, CD229, and CD84. Two major classes of SH2D1A missense mutations are identified depending on their protein half-life. Particular attention was focused on the SH2D1A T53I amino acid substitution because its ability to bind to non-phosphorylated CD150 is affected, whereas it binds normally to phosphorylated CD150. However, further studies show that T53I does not bind to receptors CD229 and CD244. The study emphasizes that SH2D1A controls multiple signal transduction pathways relevant to the pathogenesis of XLP.

EXPERIMENTAL PROCEDURES

Cells and Antibodies—COS-7 cells were cultured as described (16). The Jurkat T cell line was obtained from American Type Culture Collection. Anti-human CD150 monoclonal antibody was a gift from DNAX Research Institute (25). Anti-FLAG monoclonal antibody M5 (Eastman Kodak Co.) and rabbit anti-SHP-2 polyclonal antibody (Santa Cruz Biotechnology) were used in Western blotting. Horseradish peroxidase-conjugated goat anti-mouse and anti-rabbit IgG polyclonal antibodies were purchased from Santa Cruz Biotechnology. The anti-phosphotyrosine antibody was purchased from Zymed Laboratories Inc. The anti-mouse CD244 monoclonal antibody was purchased from Pharmingen. Anti-human CD229 (clone HCD229.1.84) and CD84 (clones CD84.1.2.21 and CD84.1.7) antibodies were produced by immunizing BALB/c mice with 300.19 murine cells stably transfected with full-length cDNA.

Plasmid Construction and Transfection—Human *SH2D1A* cDNA was cloned in vector pCMV-FLAG (Kodak) to generate a FLAG-SH2D1A construct. cDNAs coding for SH2D1A mutants based on XLP patient sequences were generated by site-directed mutagenesis in polymerase chain reactions using oligonucleotide primers incorporating the point mutation. Human WT *SH2D1A* and mutants R32Q, T53I, and T68I coding regions were cloned in vector pGEX2T (Amersham Pharmacia Biotech) to generate GST-SH2D1A constructs. The mouse *CD244* coding region was cloned in vector pcDNA3.1. The human *CD150* cDNA in vector pJFE14-SRα was a gift from DNAX Research Institute. Human *CD229* and *CD84* cDNAs were expressed by a pcDNA3.1 vector.

COS-7 cells (10×10^6) were transfected with different expression vectors containing the appropriate cDNA insert by the DEAE-dextran method (38) or using the LipofectAMINE method (Roche Molecular Biochemicals). Cells were harvested 72 h after transfection.

For cloning of rhesus monkey (*Macaca mulatta*) and cotton-top tamarin (*Saguinus oedipus*) *SH2D1A*, total mRNA was extracted from peripheral blood lymphocytes using the Trizol extraction method (Life Technologies, Inc.). Oligonucleotides based on the 5′-untranslated (forward, GCC TGG TGG ACT CTT GG) and 3′-untranslated (reverse, GAA CTG TAT TAT CTA CAA TAT ATA AGA C) regions of human *SH2D1A* were generated and used to amplify monkey *SH2D1A* cDNA by reverse transcription-polymerase chain reaction. Products were subcloned in a TA cloning vector (TA cloning kit, Invitrogen) and sequenced.

Immunoprecipitation and Western Blotting—After lysis of the cells with 0.5% CHAPS, immunoprecipitations were done using the indicated antibodies and 30 μl of protein G-agarose beads for 2 h at 4 °C. Proteins were separated by SDS-polyacrylamide gel electrophoresis and transferred to polyvinylidene difluoride membrane (Immobilon, Millipore Corp.). Filters were blocked for 1 h with 5% skim milk (or 3% bovine serum albumin) and then probed with the indicated antibodies. Bound antibody was revealed using horseradish peroxidase-conjugated secondary antibodies by enhanced chemiluminescence (Supersignal, Pierce). For anti-phosphotyrosine blotting, we used a directly conjugated horseradish peroxidase/antibody mixture (Zymed Laboratories Inc.).

Pulse-Chase Assay—Transfected COS-7 cells were starved for methionine and cysteine for 1 h and then pulse-labeled for 3 h with [^{35}S]methionine and [^{35}S]cysteine using Tran^{35}S-label (ICN Radiochemicals, Cleveland, OH) (39). Newly synthesized proteins were chased for various times in complete medium containing cycloheximide (final concentration of 25 μg/ml). Cell aliquots (5×10^6 cells/lane) were lysed, and the fate of radiolabeled SH2D1A was analyzed by immunoprecipitation with the M5 antibody to FLAG. SDS-polyacrylamide gel electrophoresis was performed using 15% density. Gels were fixed and incubated with Amplify (Amersham Pharmacia Biotech) before autoradiography.

Fluorescence Polarization Binding Assay—Interactions between GST-SH2D1A proteins and a synthetic fluorescent peptide of 11 amino acids (KSLTIpYAQVQK) corresponding to residues 276–286 of human CD150 were measured in a fluorescence polarimeter according to Danliker *et al.* (40). Polarization values were determined in a Beacon system and were expressed in millipolarization units. Before performing equilibrium binding experiments, the time to reach equilibrium was determined. Under the conditions used, the time required was <2 min (data not shown). Equilibrium binding isotherms were constructed by titrating a fixed concentration of fluorescent peptide (below the probable k_D) with increasing amounts of the GST-SH2D1A mutant chimeric proteins. The same data were also used to construct a Klotz plot (millipolarization units *versus* log[GST-SH2D1A mutants]). The curves were fit by nonlinear regression using Prism curve-fitting software (GraphPAD Software, San Diego, CA).

RESULTS

Single Amino Acid Substitutions Affect the Stability of the SH2D1A Protein—One XLP patient was found to carry a mutation in the 3′-splice acceptor of the second intron of *SH2D1A*, determining an inefficiency in mRNA processing (16). Because of this mutation, only 5–10% of WT mRNA was present in the patient's T cells, whereas most of the *SH2D1A* mRNA did not contain exon 2 (16). This prompted us to investigate whether missense mutations can affect the stability of the SH2D1A protein and thus the SH2D1A level in the cell, leading to a disease phenotype. To test this hypothesis, the protein half-lives of 10 mutant SH2D1A proteins (Y7C (βA2), S28R (βB1), R32T (βB5), C42W (βC4), T53I (βD4), T68I (βE6), Q99P, P101L (βG2), V102G (βG3), and Stop128R (tail)) (Fig. 1) were determined. The location of each mutation in the three-dimensional structure of the protein (33) is indicated in parentheses. These mutations exclusively correspond to amino acid residues that are highly conserved in human, rhesus monkey (GenBank™/EBI accession number AF322912), cotton-top tamarin (accession number AF322913), and mouse *SH2D1A* genes (Fig. 1).

Specifically, COS-7 cells were transiently transfected with *SH2D1A* cDNAs (WT or mutant) in a FLAG-tagged vector and

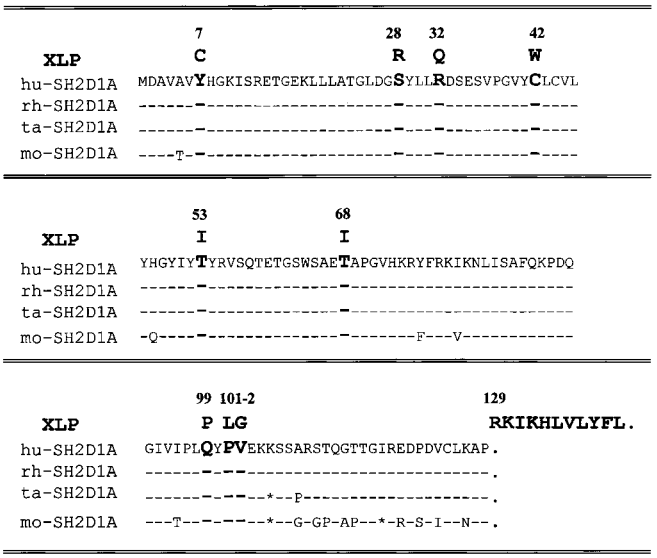

FIG. 1. **Locations of missense mutations in the SH2D1A protein sequence.** The SH2D1A coding regions of different species and XLP patient missense mutations analyzed in this work are reported. Missense mutations found in XLP patients are located in residues that are fully conserved between human, rhesus monkey, cotton-top tamarin, and mouse SH2D1A coding regions. *hu*, human; *rh*, rhesus monkey; *ta*, cotton-top tamarin; *mo*, mouse. XLP patient amino acid substitutions are indicated above the sequences (Y7C (βA2), S28R (βB1), R32T (βB5), C42W (βC4), T53I (βD4), T68I (βE6), Q99P, P101L (βG2), V102G (βG3), and Stop128R (tail)). Conserved amino acid positions in the human homologous sequences are indicated by *dashes*. Residues that are lacking in the cotton-top tamarin and mouse homolog sequences are indicated with *asterisks*.

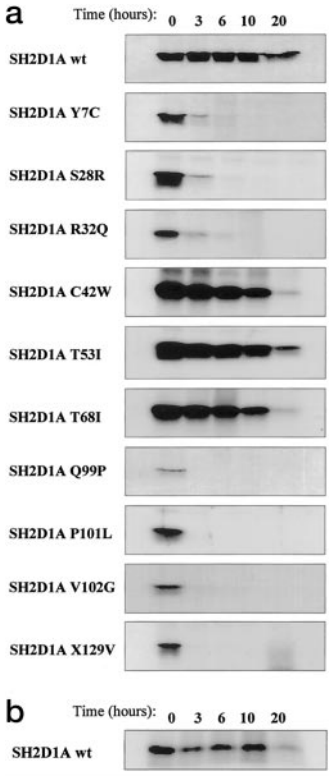

FIG. 2. **Determination of mutant SH2D1A protein half-lives.** *a*, determination of mutant SH2D1A protein half-lives in COS-7 cells. Mutant SH2D1A protein half-lives were determined as described under "Experimental Procedures." Each panel shows an autoradiograph of [^{35}S]methionine- and [^{35}S]cysteine-labeled SH2D1A at different times (0, 3, 6 10, and 20 h) after removal of the protein synthesis inhibitor cycloheximide. Mutant designations are indicated to the left of each panel. As evident, most of the mutant proteins presented extremely shortened half-lives, whereas three of them (C42W, T53I, and T68I) maintained stability comparable to that of the WT protein. *b*, determination of SH2D1A protein half-life in the Jurkat T cell line.

metabolically labeled with [^{35}S]methionine and [^{35}S]cysteine for 3 h. The cells were then incubated in medium containing cycloheximide and nonradioactive amino acids for the indicated time intervals (0, 3, 6, 10, and 20 h) (Fig. 2*a*). The half-life of the WT SH2D1A protein was also measured in the Jurkat T cell line (Fig. 2*b*). Jurkat cells were labeled under the same conditions, and the endogenous SH2D1A protein was immunoprecipitated. Fig. 2*b* shows that the half-life of T cell endogenous SH2D1A is comparable to that measured in the COS-7 cell assay (Fig. 2*a*).

When FLAG-tagged proteins were immunoprecipitated and analyzed by SDS-polyacrylamide gel electrophoresis (Fig. 2*a*), a number of missense mutations were found to dramatically shorten the half-life of SH2D1A. This was readily detectable because the WT SH2D1A protein was stable with an apparent half-life of ~18 h (Fig. 2*a*, *first panel*). The half-lives of three mutant SH2D1A proteins (C42W, T53I, and T68I) were unaffected by the mutation, whereas the majority of the amino acid substitutions resulted in an extremely shortened protein half-life (Fig. 2*a*). Inspection of the SH2D1A three-dimensional structure (33) indicated that most of the amino acid substitutions that affect protein half-life localized to the backbone of the SH2D1A SH2 domain. Surprisingly, the Stop129R mutant, the only point mutation outside of the SH2 domain, also had a drastically shortened half-life. Taken together, these observations support the notion that SH2D1A needs to be present in the cell at an optimal level in order to function normally.

In Vivo Binding of Selected SH2D1A Mutants to CD150—Previous experiments had shown that the tyrosine phosphatase SHP-2 binds to the cytoplasmic tail of human CD150 upon phosphorylation of its tyrosines (16). Mutational analyses showed that SHP-2 binds to phosphorylated tyrosines 281 and 327 of the cytoplasmic tail of CD150. The peptide segment around Tyr^{327} also binds SH2D1A, but this interaction appears to be more dependent upon phosphorylation of the tyrosine than the Tyr^{281} site.[2] To test whether mutant SH2D1A proteins had lost their ability to block recruitment of the tyrosine phosphatase SHP-2 to CD150, a COS-7 cell assay was used. COS-7 cells were transiently transfected with combinations of plasmids coding for SH2D1A (WT or mutant) and CD150. To phosphorylate the tyrosines in the cytoplasmic tail of CD150, a cDNA encoding the tyrosine kinase Fyn was cotransfected. After 72 h, cells were lysed, and post-nuclear lysates were immunoprecipitated with anti-CD150 antibodies. WT SH2D1A bound to both phosphorylated and non-phosphorylated CD150 and, as expected, blocked SHP-2 recruitment to phosphorylated CD150 completely (Fig. 3*A*, *lanes 3* and *4*). Almost all SH2D1A mutants had lost their ability to block SHP-2 recruitment; as expected, the proteins that had shortened half-lives belonged to this group (data not shown).

Two mutants that disrupt the phosphotyrosine-binding pocket of SH2D1A were analyzed. Mutant R32Q, which was predicted to affect interactions with both the Tyr(P)^{281} and Tyr^{281} peptides (33), was unable to bind the phosphorylated and non-phosphorylated CD150 proteins (Fig. 3*A*, *lanes 5* and *6*). R32Q also completely failed to block SHP-2 recruitment. Because mutant R32Q does not only have a mutation that grossly disrupts binding to phosphorylated and non-phosphorylated CD150, as R32Q is present in reduced copies in the cell, its lack of SHP-2 competition is likely to be the result of both properties. By contrast, mutant C42W is a relatively stable

[2] D. Howie and C. Terhorst, submitted for publication.

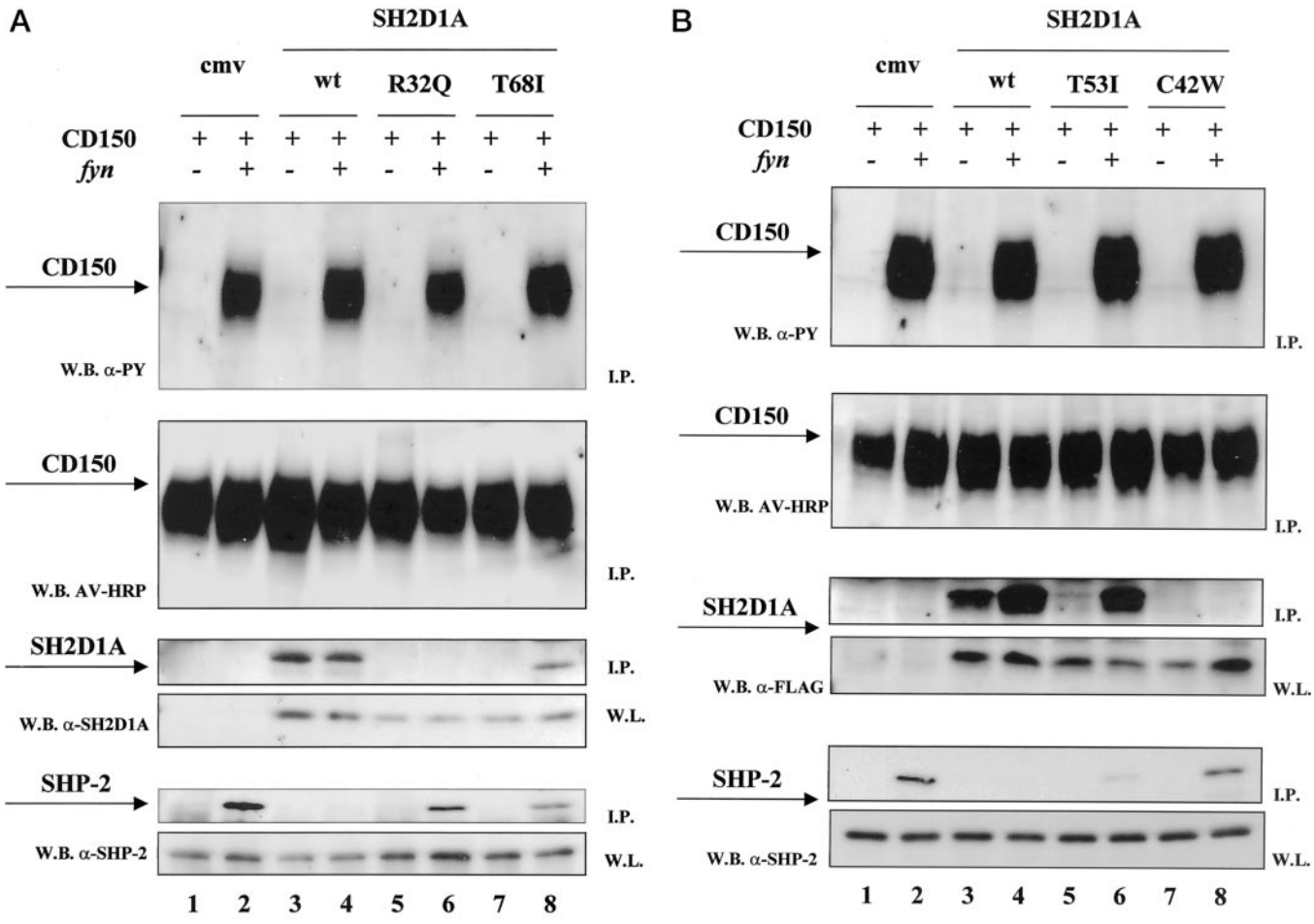

FIG. 3. **Analysis of *in vivo* binding of SH2D1A mutants to the CD150 receptor.** *In vivo* interactions were examined after cotransfection of combinations of WT SH2D1A or mutant proteins R32Q, C42W, T53I, and/or T68I (in pCMV-FLAG) with human CD150 into COS-7 cells. Combinations of cDNAs used in the transfections are indicated above *panels a* and *b* (+, transfection of the indicated molecule; −, transfection with an equal amount of empty vector). A cDNA encoding human Fyn was cotransfected as indicated (+). In the *lanes 1* and *2* of each panel, an equal amount of pCMV-FLAG empty vector (*cmv*) was used. *I.P.*, immunoprecipitate; *W.L.*, whole lysate. All cells were biotinylated prior to subjection to detergent lysis. Cell lysates (1×10^7 cell eq) were subjected to immunoprecipitation with monoclonal antibody recognizing CD150. Samples were analyzed by Western blotting (*W.B.*) with anti-phosphotyrosine antibody (*α-PY*), horseradish peroxidase-conjugated avidin (*AV-HRP*), anti-FLAG antibody, and anti-SHP-2 antibody, as indicated to the left of each panel. *A*, SH2D1A R32Q and T68I binding to CD150; *B*, SH2D1A C42W and T53I binding to CD150.

protein (Fig. 2*a*), and its position in the SH2D1A structure predicts that it could also interfere with binding to both phosphorylated and non-phosphorylated CD150. This is indeed the case, as shown in Fig. 3*B* (*lanes 7* and *8*). This lack of binding is therefore consistent with an important role for Cys^{42} in the interactions with the CD150 tyrosine site.

A second stable mutant protein (T68I) did bind phosphorylated CD150, but not the non-phosphorylated CD150 protein (Fig. 3*A*, *lanes 7* and *8*). However, its ability to block SHP-2 binding to phosphorylated CD150 was reduced. This mutation affects the interaction of Val^{284} at position +3 of the CD150 peptide with the hydrophobic cleft of SH2D1A. Taken together, the COS-7 *in vivo* protein binding experiments emphasized the importance of SH2D1A protein stability in blocking recruitment of SHP-2. Moreover, as predicted from the structure of the SH2D1A SH2 domain, mutations that affect the tyrosine-binding pocket or the hydrophobic cleft of SH2D1A reduce the affinity of the mutant protein for both phosphorylated and non-phosphorylated CD150.

One of the stable mutants of SH2D1A found in XLP patients displayed an unexpected *in vivo* binding pattern. As shown in Fig. 3*B* (*lane 5*), mutant T53I failed to bind to non-phosphorylated CD150 in COS-7 cells. However, its ability to bind CD150 after phosphorylation was preserved, and the T53I protein excluded the tyrosine phosphatase SHP-2 from its docking site in CD150 (Fig. 3*B*, *lane 6*). Because of this unique binding pattern, T53I was studied further.

Mutation T53I in SH2D1A Selectively Disrupts Binding to the Non-phosphorylated Form of the CD150 Tyr^{281} Peptide—Binding of SH2D1A T53I to the CD150 Tyr^{281} and $Tyr(P)^{281}$ peptides was compared with the binding of WT SH2D1A to the same peptides by fluorescence polarization. For these experiments, an 11-mer amino acid peptide encompassing CD150 cytoplasmic region 276–286 was labeled with fluorescein isothiocyanate in its α-amino group. This peptide, which represents the major SH2D1A-binding site in CD150, was used previously for fluorescence polarization studies with WT SH2D1A (34). Binding of this peptide to SH2D1A (either in the presence or absence of CD150 Tyr^{281} phosphorylation) was determined by incubating varying concentrations of GST-SH2D1A with the peptides. As shown in Fig. 4*a*, SH2D1A T53I bound to the phosphorylated peptide with an affinity comparable to that of the WT protein (k_D = 0.25 μM) (Fig. 4*c*). By contrast, SH2D1A T53I bound the non-phosphorylated peptide with a significantly decreased affinity (k_D = 8.7 μM) (Fig. 4, *b* and *c*).

In a parallel study, the SH2D1A T68I mutant protein was also assayed for peptide binding using fluorescence polariza-

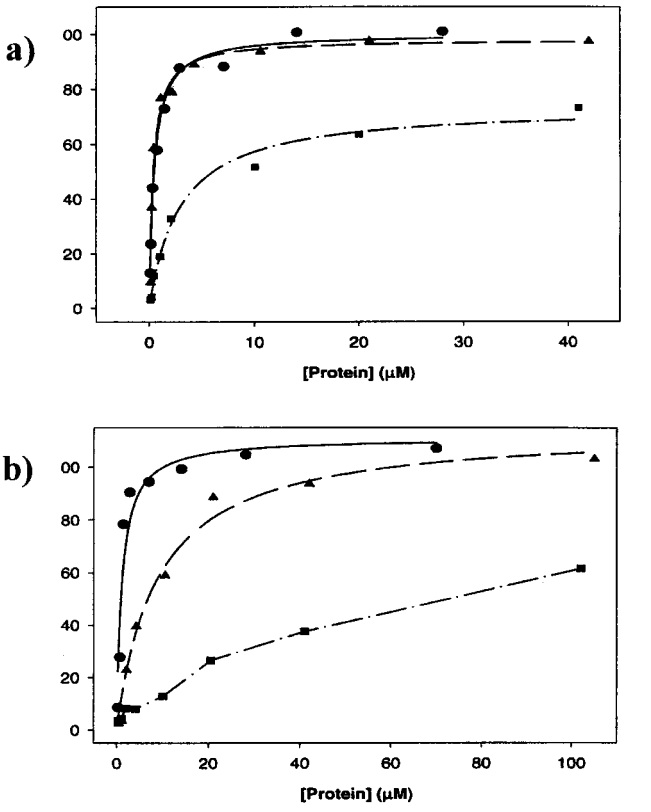

c)

	SH2D1A wt	SH2D1A T53I	SH2D1A T68I
n-pY-c	0.23 +/- 0.03	0.25 +/- 0.03	5.08 +/-1.92
n-Y-c	0.60 +/- 0.21	8.70 +/- 1.45	> 100

FIG. 4. ***In vitro* binding of SH2D1A mutants T53I and T68I to a CD150 peptide.** Fluorescence polarization measurements of the interaction between scalar concentrations of GST-WT SH2D1A, GST-SH2D1A T53I, or GST-SH2D1A T68I and a 11-mer synthetic peptide identical to amino acids 276–287 of human CD150 are shown. The peptide tyrosine residue was either phosphorylated or not ($Tyr(P)^{281}$ or Tyr^{281}); a fluorescein group was attached to the α-NH_2 group of each peptide. *a*, GST-WT SH2D1A (●), GST-SH2D1A T53I (▲), or GST-SH2D1A T68I (■) binding to $Tyr(P)^{281}$. *b*, GST-WT SH2D1A (●), GST-SH2D1A T53I (▲), or GST-SH2D1A T68I (■) binding to Tyr^{281}. *x axes*, protein concentration (μM); *y axes*, polarization unit (*mP*). *c*, summary of the apparent dissociation constant (k_D) of WT SH2D1A and the T53I and T68I mutants for each peptide calculated as described under "Experimental Procedures."

tion. T68I displayed a dramatically reduced affinity for the phosphorylated peptide (k_D = 5.08 μM) (Fig. 4, *a* and *c*), whereas it failed completely to bind the non-phosphorylated peptide (Fig. 4, *b* and *c*). Thus, mutant T68I is incapable of binding to CD150 Tyr^{281} in both the phosphorylated and non-phosphorylated states.

Structural Modeling of the SH2D1A T53I Mutant—High affinity association of SH2 domains with Tyr-containing motifs depends upon phosphorylation of the Tyr embedded in the ligand motif. The SH2 domain of SH2D1A represents the first example of an SH2 domain able to bind a motif in the absence of tyrosine phosphorylation. The three-pronged modality of SH2D1A binding to CD150 was originally proposed as responsible for its ability to block recruitment of SH2 domain-containing adapters and enzymes. Because our results indicate that the SH2D1A T53I mutant selectively interferes with CD150 binding in the absence of Tyr^{281} phosphorylation, a structural

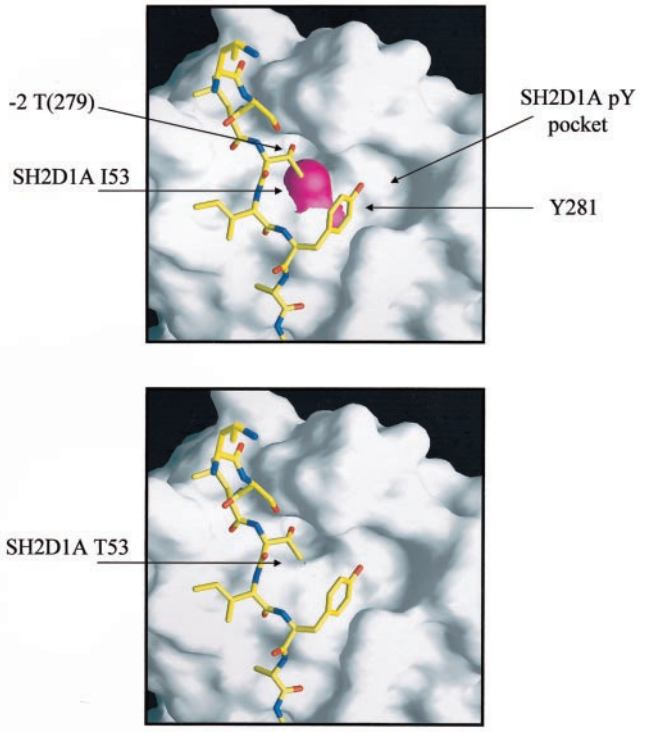

FIG. 5. **Structural modeling of the interaction between the SH2D1A T53I mutant and the CD150 Tyr^{281} cytoplasmic tail peptide.** The surface representations of SH2D1A T53I (*upper panel*) and WT SH2D1A (*lower panel*) are shown. *Arrows* indicate the Tyr(P) pocket in SH2D1A, position 53 in SH2D1A (*violet* in SH2D1A T53I), and Thr^{279} and Tyr^{281} of the CD150 peptide. The bound peptide is shown in a *stick* representation (*yellow*). Replacement of Thr^{53} by isoleucine severely affects the binding pocket for Thr^{279} (position −2) of the CD150 peptide, severely impairing the SH2D1A/non-phosphorylated CD150 interaction.

model for T53I was generated based on the structure of SH2D1A (33). To this purpose, the structure of the SH2D1A SH2 domain was altered by substituting Thr^{53} with isoleucine. A model of the SH2D1A T53I mutant SH2 domain in complex with the CD150 Tyr^{281} peptide is shown in Fig. 5. Replacement of Thr^{53} with isoleucine eliminates the binding pocket for Thr at position −2 (Thr^{279}) of CD150. This prevents the interaction of Thr at position −2 with a buried water molecule and with Glu^{17}, thus blocking interactions of one of the amino acids located N-terminal to Tyr^{281}. Thus, this selective amino acid substitution changes the unique SH2 domain of SH2D1A into a more conventional SH2 domain structure that predominantly binds to a phosphorylated state of the ligand.

Binding to CD229, CD244, and CD84—In addition to CD150, SH2D1A binds to at least three other transmembrane glycoproteins of the CD150 family: CD244 (2B4) (19, 20), CD229 (Ly-9), and CD84 (21). Therefore, mutants C42W, T53I, and T68I were tested for their ability to bind to these receptors. COS-7 cells were transiently transfected with combinations of plasmids coding for SH2D1A (WT or mutant) and CD244 (Fig. 6, *A* and *B*), CD84 (Fig. 6*C*), or CD229 (Fig. 6*D*). *Lanes 1* and *2* in Fig. 6 (*A–D*) are the negative controls (where a FLAG-tagged empty vector was used), whereas in *lanes 3* and *4*, a FLAG-tagged WT SH2D1A vector was used as a positive control.

Compared with WT SH2D1A, binding of SH2D1A mutants C42W (Fig. 6*A*, *lanes 5* and *6*), T53I (Fig. 6*A*, *lanes 7* and *8*), and T68I (Fig. 6*B*, *lanes 5* and *6*) to the CD244 receptor was totally disrupted. Binding of these mutants to CD84 (Fig. 6*C*) and CD229 (Fig. 6*D*) was also severely impaired, albeit that of mutant T53I preserved a marginal binding to CD84 (Fig. 6*C*, *lanes 9* and *10*). These results indicate that amino acid substi-

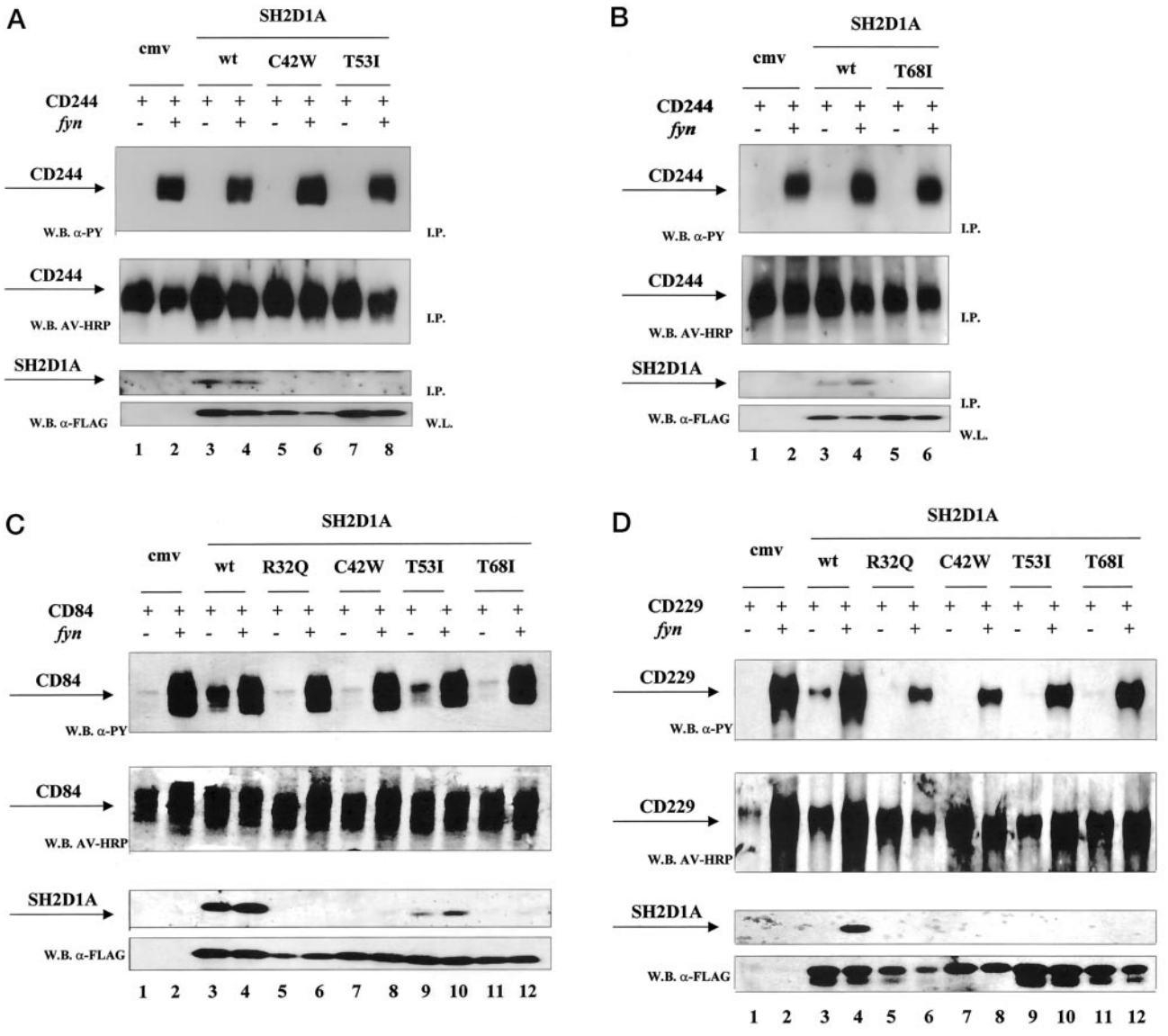

FIG. 6. **Analysis of *in vivo* binding of SH2D1A mutants to CD244, CD229, and CD84.** *In vivo* interactions were examined after cotransfection of combinations of WT SH2D1A or mutant proteins R32Q, C42W, T53I, and/or T68I (in pCMV-FLAG) with CD244, CD229, or CD84 into COS-7 cells. Combinations of cDNAs used in the transfections are indicated above *panels A–D* (+, transfection of the indicated molecule; −, transfection with an equal amount of empty vector). A cDNA encoding human Fyn was cotransfected as indicated (+). In *lanes 1* and *2* of each *panel,* an equal amount of pCMV-FLAG empty vector (*cmv*) was used. *I.P.*, immunoprecipitate; *W.L.*, whole lysate. All cells were biotinylated prior to subjection to detergent lysis. Cell lysates (1×10^7 cell eq) were subjected to immunoprecipitation with monoclonal antibody recognizing the CD150-related surface receptors. Samples were analyzed by Western blotting (*W.B.*) with anti-phosphotyrosine antibody (*α-PY*), horseradish peroxidase-conjugated avidin (*AV-HRP*), anti-FLAG antibody, and anti-SHP-2 antibody, as indicated to the left of each panel. *A*, SH2D1A C42W and T53I binding to CD244; *B*, SH2D1A T68I binding to CD244; *C*, SH2D1A R32Q, C42W, T53I, and T68I binding to CD84; *D*, SH2D1A R32Q, C42W, T53I, and T68I binding to CD229.

tutions that disrupt the Tyr(P)-binding pocket (R32Q and C42W) or that interfere with the recognition of residues at positions −2 (Thr) and +3 (Val) of the binding motif (T53I and T68I, respectively) differentially compromise SH2D1A binding to CD150-related receptors.

DISCUSSION

The *SH2D1A* gene encodes a single SH2 domain protein involved in signal transduction events in T lymphocytes. The availability of missense mutations throughout the *SH2D1A* sequence provides a useful tool to dissect SH2 domain structure/function relationships. This study represents the analysis of 10 single amino acid substitutions found in XLP patients. Each of these mutation affects an amino acid residue that is conserved among different species: human, rhesus monkey, cotton-top tamarin, and mouse (Fig. 1).

A summary of the SH2D1A biochemical characterization is shown in Table I. The missense mutations of SH2D1A are clustered into two major groups according to their effect on protein stability and binding to the receptors. A structural evaluation of the mutations allows further classification (Fig. 7). The two protein groups are determined by 1) protein instability, as judged by a substantially decreased half-life (*e.g.* mutants Y7C, S28R, Q99P, P101L, V102G, and X129R), or 2) an impaired ability of binding to CD150 and CD150-related receptors while maintaining protein stability (*e.g.* C42W, T53I, and T68I). The SH2D1A R32Q mutant belongs to both groups, as its failure to bind CD150-related receptors is accompanied by a substantially decreased half-life.

Group 1 mutants are all in principle capable of binding to the CD150 motif via a three-pronged interaction. The observation that some of them (*i.e.* P101L and Stop129R) are capable of binding the CD150 peptide *in vitro* (data not shown) while

TABLE I
Summary of SH2D1A mutant biochemical characterization

⇓⇓, highly decreased half-life; =, half-life similar to that of WT SH2D1A; ND, not determined; −, absence of binding; +, presence of binding; ±, weak binding.

	SH2D1A									
	Y7C	S28R	R32Q	C42W	T53I	T68I	Q99P	P101L	V102G	X128R
Half-life	⇓⇓	⇓⇓	⇓⇓	=	=	=	⇓⇓	⇓⇓	⇓⇓	⇓⇓
Binding to:										
CD150	ND	ND	−	−	+	±	ND	ND	ND	ND
CD244	ND	ND	ND	−	−	−	ND	ND	ND	ND
CD229	ND	ND	−	−	−	−	ND	ND	ND	ND
CD84	ND	ND	−	−	±	−	ND	ND	ND	ND

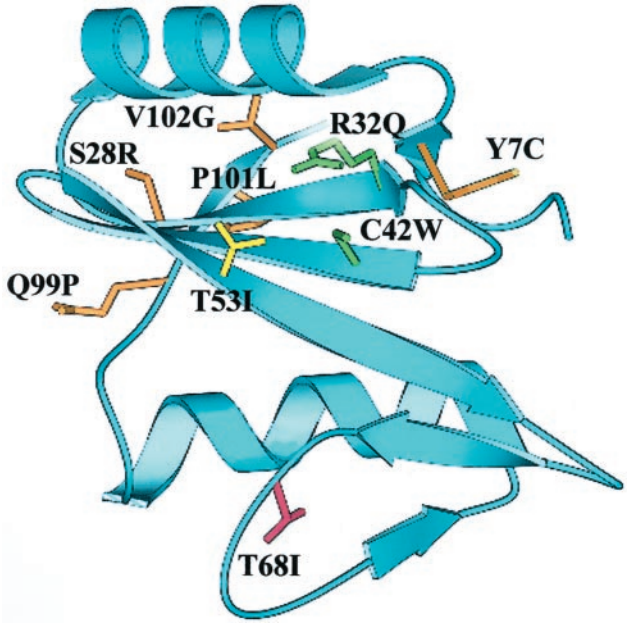

FIG. 7. **Ribbon diagram of the SH2D1A SH2 domain with the locations of the XLP amino acid substitutions studied in this work.** A ribbon diagram of the SH2D1A SH2 domain is represented. Lateral chains of amino acid positions where missense mutations have been identified in XLP patients are colored accordingly to the type of biochemical/structural alteration identified (*brown*, missense mutations leading to protein instability with severely decreased protein half-life; *green*, missense mutations leading to a disruption of the phosphotyrosine-binding pocket; *yellow*, missense mutation interfering with C-terminal motif interactions; *violet*, missense mutation interfering with N-terminal motif interactions).

failing to block recruitment of SHP-2 in the COS-7 cells indicates that there is a threshold level of SH2D1A in the cell below which a propensity for XLP develops. This is consistent with the partially defective transcription of *SH2D1A* in an XLP patient who has a mutation in the 5′-splice acceptor site of the second exon (16). This XLP patient still produces 5–10% of WT *SH2D1A* mRNA, which must result in a below threshold protein level (16). A limited amount of a WT protein may therefore lead to the pathogenesis of XLP, strongly supporting the notion that SH2D1A acts as a natural inhibitor. Group 1 mutants contain also a protein with an amino acid substitution located outside of the SH2 domain sequence. This mutant contains an SH2D1A tail prolonged by an additional 11 residues because of a mutation that transforms the stop codon to an arginine. At first, we assumed that the SH2D1A tail might have a significant, yet unknown, functional role. Surprisingly, pulse-chase labeling experiments showed, however, that the additional amino acids provide a degradation signal resulting in a shortened half-life of the protein. Therefore, this mutant also falls in the first category. Its degradation could not directly involve the ubiquitin system because it lacks a known recognition site for the ubiquitin system. However, the additional 11-amino acid sequence contained a PDZ recognition motif, which might serve as a link to a protein degradation system (Scansite Software).

Group 2 mutants are stable but functionally inefficient proteins due to a decreased ability to interact with CD150-related receptors. Two mutants, C42W and T68I, do not bind to any of the four cell-surface receptors. The C42W amino acid substitution affects interactions with the classical phosphotyrosine-binding pocket as well as with the threonine residue at position −2 of the CD150 Tyr^{281} motif and consequently result in a severe loss in binding affinity. According to the SH2D1A structure (33), Thr^{68} articulates interactions with the Val residue at position +3 in the CD150 Tyr^{281} peptide. A T68I mutation thus disrupts the binding of CD150 Val^{284} to the hydrophobic cleft. This amino acid substitution points to a critical role that Val at position +3 plays in stabilizing SH2 domain interactions.

Of particular interest is the group 2 mutant T53I. Mutant T53I is unusual in that it binds in a WT fashion to the phosphorylated tail of CD150 (k_D ~250 nM) and competes against SHP-2 recruitment. However, it displayed a severely decreased binding affinity *versus* the non-phosphorylated CD150 peptide (dissociation constant of 8–9 μM). Analysis of the SH2D1A structure indicates that the isoleucine replacing Thr^{53} eliminates the binding pocket for Thr^{279} of CD150 (Thr at position −2). This prevents the interaction of Thr at position −2 with the buried water molecule and with Glu^{17}, thereby blocking interactions of one of the amino acids located N-terminal to Tyr^{281}. Whereas the SH2D1A T53I mutant still efficiently binds to phosphorylated CD150, T53I fails to efficiently bind to three other SH2D1A-interacting molecules, CD244, CD229, and CD84. These results indicate the important role that motif interactions of Tyr at position −2 play in stabilizing SH2D1A SH2 domain binding to its receptors. Conventional SH2 domains contain Ile or Leu at position βD4, which is Thr^{53} in SH2D1A. Replacing threonine by isoleucine in mutant T53I may change the unique SH2 domain of SH2D1A into a more conventional SH2 domain structure that is able to bind to a phosphotyrosine motif only. Altogether, these data suggest that the ability of SH2D1A to bind non-phosphorylated Tyr peptides (probably the most striking SH2D1A feature) depends at least partially on its peculiarity to coordinate Tyr N-terminal interactions.

All the missense mutations in the *SH2D1A* gene investigated in this study had fatal consequences for the XLP patients. The clinical analysis of several members of six families affected by *SH2D1A* missense mutations (Y7C, S28R, C42W, T53I, Q99P, and V102G) shows that for a given mutant, a combination of different phenotypes is found (Table II). In particular, we could not find significant differences in terms of onset of the disease, frequency of fatal infectious mononucleosis, median age of death, the frequency of lymphoma, and the presence or absence of EBV (Table II). Whether other elements are able to shape the clinical phenotype remains to be investigated.

In conclusion, our results indicate a correlation between different types of SH2D1A signal transduction abnormalities

TABLE II
Summary of clinical data

FIM, fatal infectious mononucleosis; LPD, lymphoproliferative disorders; dysG, dysgammaglobulinemia; AA, aplastic anemia; y, years.

	SH2D1A					
	Y7C	S28R	C42W	T53I	Q99P	V102G
Affected males in the family	3	6	5	14	17	2
Clinical phenotypes of affected males	FIM, AA	LPD, dysG	FIM, dysG	FIM, LPD, dysG	FIM, LPD, dysG	FIM
Median age of onset	8.9 y	11.18 y	8.0 y	4.5 y	7.15 y	25.6 y
Median age of survivals	No survival	33 y, two survivals	41 y, one survival	21.5 y, four survivals	35 y, five survivals	No survival

(*i.e.* stability or binding) with the location of the amino acid substitution. Taken together, the analysis of these selective alterations in the SH2D1A structure indicated two distinct mechanisms underlying the pathogenesis of XLP. First, limited amounts of SH2D1A, attributable to protein instability, lead to the disease. Second, the disruption of binding to the CD150-related receptors *per se* leads to XLP. Because these biochemical findings are not paralleled by differences in terms of XLP disease clinical phenotypes or severity, we conclude that signal transduction through CD150, CD229, CD244, and CD84 receptors is likely redundant. Additional unidentified genetic or environmental factors must account for the variability in XLP disease manifestations. Moreover, these results indicate that SH2D1A controls several distinct signal transduction pathways in T and NK cells.

Acknowledgment—We thank Kareen Hershberger (of the laboratory of Dr. N. L. Letvin) for providing primate lymphocytes.

REFERENCES

1. Purtilo, D. T., Cassel, C. K., Yang, J. P., and Harper, R. (1975) *Lancet* **1,** 935–940
2. Seemayer, T. A., Gross, T. G., Egeler, R. M., Pirruccello, S. J., Davis, J. R., Kelly, C. M., Okano, M., Lanyi, A., and Sumegi, J. (1995) *Pediatr. Res.* **38,** 471–478
3. Sullivan, J. L. (1999) *Curr. Opin. Immunol.* **11,** 431–434
4. Howie, D., Sayos, J., Terhorst, C., and Morra, M. (2000) *Curr. Opin. Immunol.* **12,** 474–478
5. Morra, M., Howie, D., Simarro-Grande, M., Sayos, J., Wang, N., Wu, C., Engel, P., and Terhorst, C. (2001) *Annu. Rev. Immunol.* **19,** 657–682
6. Nichols, K. E. (2000) *Rev. Immunogenet.* **2,** 256–266
7. Schuster, V., and Kreth, H. W. (2000) *Immunol. Rev.* **178,** 21–28
8. Grierson, H. L., Skare, J., Hawk, J., Pauza, M., and Purtilo, D. T. (1991) *Am. J. Med. Genet.* **40,** 294–297
9. Strahm, B., Rittweiler, K., Duffner, U., Brandau, O., Orlowska-Volk, M., Karajannis, M. A., Stadt, U., Tiemann, M., Reiter, A., Brandis, M., Meindl, A., and Niemeyer, C. M. (2000) *Br. J. Haematol.* **108,** 377–382
10. Brandau, O., Schuster, V., Weiss, M., Hellebrand, H., Fink, F. M., Kreczy, A., Friedrich, W., Strahm, B., Niemeye, C., Belohradsky, B. H., and Meindl, A. (1999) *Hum. Mol. Genet.* **8,** 2407–2413
11. Parolini, S., Bottino, C., Falco, M., Augugliaro, R., Giliani, S., Franceschini, R., Ochs, H., Wolf, H., Bonnefoy, J. Y., Biassoni, R., Moretta, L., Notarangelo, L. D., and Moretta, A. (2000) *J. Exp. Med.* **3,** 337–346
12. Benoit, L., Wang, X., Pabst, H. F., Dutz, J., and Tan, R. (2000) *J. Immunol.* **165,** 3549–3553
13. Lanier, L. L. (1998) *Annu. Rev. Immunol.* **16,** 359–393
14. Tangye, S. G., Phillips, J. H., Lanier, L. L., and Nichols, K. E. (2000) *J. Immunol.* **165,** 2932–2936
15. Coffey, A. J., Brooksbank, R. A., Brandau, O., Oohashi, T., Howell, G. R., Bye, J. M., Cahn, A. P., Durham, J., Heath, P., Wray, P., Pavitt, R., Wilkinson, J., Leversha, M., Huckle, E., Shaw-Smith, C. J., Dunham, A., Rhodes, S., Schuster, V., Porta, G., Yin, L., Serafini, P., Sylla, B., Zollo, M., Franco, B., *et al.* (1998) *Nat. Genet.* **20,** 129–135
16. Sayos, J., Wu, C., Morra, M., Wang, N., Zhang, X., Allen, D., van Schaik, S., Notarangelo, L., Geha, R., Roncarolo, M. G., Oettgen, H., de Vries, J. E., Aversa, G., and Terhorst, C. (1998) *Nature* **395,** 462–469
17. Nichols, K. E., Harkin, D. P., Levitz, S., Krainer, M., Kolquist, K. A., Genovese, C., Bernard, A., Ferguson, M., Zuo, L., Snyder, E., Buckler, A. J., Wise, C., Ashley, J., Lovett, M., Valentine, M. B., Look, A. T., Gerald, W., Housman, D. E., and Haber, D. A. (1998) *Proc. Natl. Acad. Sci. U. S. A.* **95,** 13765–13770
18. Nagy, N., Cerboni, C., Mattsson, K., Maeda, A., Gogolak, P., Sumegi, J., Lanyi, A., Szekely, L., Carbone, E., Klein, E., and Klein, G. (2000) *Int. J. Cancer* **88,** 439–447
19. Tangye, S. G., Lazetic, S., Woollatt, E., Sutherland, G. R., Lanier, L. L., and Phillips, J. H. (1999) *J. Immunol.* **162,** 6981–6985
20. Sayos, J., Nguyen, K. B., Wu, C., Stepp, S. E., Howie, D., Schatzle, J. D., Kumar, V., Biron, C. A., and Terhorst, C. (2000) *Int. Immunol.* **12,** 1749–1757
21. Sayos, J., Martin, M., Chen, A., Simarro, M., Howie, D., Morra, M., Engel, P., and Terhorst, C. (2001) *Blood* **97,** 3867–3874
22. Lewis, J., Eiben, L. J., Nelson, D. L., Cohen, J. I., Nichols, K. E., Ochs, H. D., Notarangelo, L. D., and Duckett, C. S. (2001) *Clin. Immunol.* **100,** 15–23
23. Wang, N., Morra, M., Wu, C., Gullo, C., Howie, D., Coyle, T., Engel, P., and Terhorst, C. (2001) *Immunogenetics* **53,** 382–394
24. Aversa, G., Carballido, J., Punnonen, J., Chang, C. C., Hauser, T., Cocks, B. G., and de Vries, J. E. (1997) *Immunol. Cell Biol.* **75,** 202–205
25. Cocks, B. G., Chang, C. C., Carballido, J. M., Yssel, H., de Vries, J. E., and Aversa, G. (1995) *Nature* **376,** 260–263
26. Castro, A. G., Hauser, T. M., Cocks, B. G., Abrams, J., Zurawski, S., Churakova, T., Zonin, F., Robinson, D., Tangye, S. G., Aversa, G., Nichols, K. E., de Vries, J. E., Lanier, L. L., and O'Garra, A. (1999) *J. Immunol.* **163,** 5860–5870
27. Mavaddat, N., Mason, D. W., Atkinson, P. D., Evans, E. J., Gilbert, R. J. C., Stuart, D. I., Fennelly, J. A., Barclay, A. N., Davis, S. J., and Brown, M. H. (2000) *J. Biol. Chem.* **275,** 28100–28109
28. Tatsuo, H., Ono, N., Tanaka, K., and Yanagi, Y. (2000) *Nature* **406,** 893–897
29. Nakajima, H., and Colonna, M. (2000) *Hum. Immunol.* **61,** 39–43
30. Brown, M. H., Boles, K., van der Merwe, P. A., Kumar, V., Mathew, P. A., and Barclay, A. N. (1998) *J. Exp. Med.* **188,** 2083–2090
31. Latchman, Y., McKay, P. F., and Reiser, H. (1998) *J. Immunol.* **161,** 5809–5812
32. Sylla, B. S., Murphy, K., Cahir-McFarland, E., Lane, W. S., Mosialos, G., and Kieff, E. (2000) *Proc. Natl. Acad. Sci. U. S. A.* **97,** 7470–7475
33. Poy, F., Yaffe, M. B., Sayos, J., Saxena, K., Morra, M., Sumegi, J., Cantley, L. C., Terhorst, C., and Eck, M. J. (1999) *Mol. Cell* **4,** 555–561
34. Li, S.-C., Gish, G., Yang, D., Coffey, A. J., Forman-Kay, J. D., Ernberg, I., Kay, L. E., and Pawson, T. (1999) *Curr. Biol.* **9,** 1355–1362
35. Tangye, S. G., Phillips, J. H., and Lanier, L. L. (2000) *Semin. Immunol.* **12,** 149–157
36. de la Fuente, M. A., Tovar, V., Villamor, N., Zapater, N., Pizcueta, P., Campo, E., Bosch, J., and Engel, P. (2001) *Blood* **97,** 3513–3520
37. Sumegi, J., Huang, D., Lanyi, A., Davis, J. D., Seemayer, T. A., Maeda, A., Klein, G., Seri, M., Wakiguchi, H., Purtilo, D. T., and Gross, T. G. (2000) *Blood* **96,** 3118–3125
38. Ausubel, F. M., Brent, R., Kingston, R. E., Moore, D. D., Seidman, J. G., Smith, J. A., and Struhl, K. (1995) *Current Protocols in Molecular Biology*, Suppl. 17, p. 16.13.1, Wiley, New York
39. Hall, C., Berkhout, B., Alarcon, B., Sancho, J., Wileman, T., and Terhorst, C. (1991) *Int. Immunol.* **3,** 359–368
40. Danliker W. B., Levin J., and Rao B. R. (1981) *Methods Enzymol.* **74,** 3–28

Characterization of *SH2D1A* Missense Mutations Identified in X-linked Lymphoproliferative Disease Patients

Massimo Morra, Maria Simarro-Grande, Margarita Martin, Alice Siau-In Chen, Arpad Lanyi, Olin Silander, Silvia Calpe, Jack Davis, Tony Pawson, Michael J. Eck, Janos Sumegi, Pablo Engel, Shun-Cheng Li and Cox Terhorst

J. Biol. Chem. 2001, 276:36809-36816.
doi: 10.1074/jbc.M101305200 originally published online July 26, 2001
